Journal of Japan Association for Earthquake Engineering, Vol. 23, No. 3, 2023

STUDY OF SITE-SPECIFIC EARTHQUAKE GROUND MOTION EVALUATION MODELS USING MACHINE LEARNING CONSIDERING EPICENTRAL DIRECTION AND RESPONSE DURATION TIME

Toru ISHII[1] and Atsuko OANA[2]

[1] Member, Dr. Eng., Senior Research Expert, Institute of Technology, Shimizu Corporation, Tokyo, Japan, tokyo@shimz.co.jp
[2] Member, Dr. Eng., Researcher, Institute of Technology, Shimizu Corporation, Tokyo, Japan, a.oana@shimz.co.jp

ABSTRACT: To acquire new knowledge through earthquake ground motion evaluation from a new perspective, the authors attempted to create a site-specific earthquake ground motion evaluation model by machine learning using earthquake ground motion records obtained in the past as training data. The epicentral direction and response duration time of the earthquake ground motion, which had not been addressed by conventional attenuation relations, were also examined. Overall, the observed values were evaluated and modeled well, within twice to half the observed values. The average ratio of the evaluated value to the observed value was approximately 1, and the common logarithmic standard deviation was slightly greater than 0.2 for the amplitude of ground motion and slightly greater than 0.1 for the response duration time. The impact of the epicentral direction on the response duration time was large, and in some cases, it was almost equal to or greater than the impact of each parameter in the conventional prediction equations.

Keywords: *Earthquake ground motion evaluation, Machine learning, Epicentral direction, Duration time*

1. INTRODUCTION

In recent years, seismic observation stations have been established across Japan to obtain large amounts of high-quality data in real time[e.g.1)], and remarkable advances in computers have made it possible to process these data at high speed. Such rapid changes in the data, information, and computer environment provide great potential for dramatic development of both the quality and the quantity of knowledge pertaining to earthquakes and ground motions. Additionally, through attempts to improve earthquake ground motion evaluation models (attenuation relations, etc.), many general and practical equations based on regression analyses have been developed and used[e.g.2)], but the data and information on which they are based include biases in the number of earthquakes occurring because of the source regions and biases in the number of records depending on observation sites, so some misrepresentation is included in the models. Furthermore, every time a large-scale earthquake disaster has occurred, researchers have noticed that the approach and results of the research contain preconceptions and assumptions attributable

to expert opinion. In particular, conventional earthquake ground motion prediction equations implement sources, propagations, and site characteristics that are seemingly physical but are often simplified or consolidated. Although it is possible to improve these in the future, there are limitations. There are also technical problems because nonlinear interrelationships left unaddressed exist between parameters, although they may be explained in some way by the data. The rapid increase in data and information that has occurred in recent years should be a great help in resolving this problem; however, because of the fragmentation and sophistication of specialized fields, there is a limit to the amount of time and effort available from specialists. To overcome this circumstance, it is necessary to entrust the work that can be automatically processed to computers so that people can fully devote their time and effort to advanced and detailed examination and the various decisions that they should embrace.

From this point of view, for a satisfying future environment, a ground motion evaluation model should be automatically generated, verified, and upgraded by artificial intelligence (AI) implementing big data, such as observation data obtained each time an earthquake occurs. Recently, pioneering efforts have been made to construct earthquake ground motion prediction models using machine learning[3)–10)]. This study performed a preliminary examination of constructing an earthquake ground motion evaluation model using machine learning to understand how new knowledge about earthquake ground motion might be acquired and implemented when such an environment is realized in the future.

This study aimed to acquire new understandings from the following perspectives. First, considering the great benefits of making most effective use of AI and big data, as one of the specific targets, an earthquake ground motion evaluation model was constructed for each observation station where a large number of high-quality observation records and site-specific ground information were obtained. Second, it has been pointed out that observation records show differences in earthquake ground motion characteristics depending on the epicentral direction[e.g.11), 12)]. These results reflect the differences in earthquake occurrence frequency and source characteristics in multiple focal regions, as well as differences in three-dimensional seismic wave propagation characteristics. Moreover, nonlinear interrelationships exist among these multiple factors, making them difficult to model with conventional simple equations. However, it is possible that these problems may be explained by some data process if the new technology of machine learning were used, so characteristics depending on epicentral direction were also evaluated in this study. Third, the time-dependent characteristics of earthquake ground motions, such as the duration time, and the amplitude and periodic characteristics, response spectrum, etc., are important factors for understanding the phenomena and also for seismic engineering[13)]. However, they have not been considered in most conventional attenuation relationships. Therefore, this study also evaluated the response duration time[14)] of earthquake ground motion.

2. EXAMINATION METHOD AND DATA USED

This study created earthquake ground motion evaluation models through machine learning[15)] using ground motion observation records obtained in the past as training data. It is possible to create a machine-learning model that associates the parameters describing the source and propagation characteristics as feature parameters and the earthquake motion indices obtained from observation records as target variables.

Table 1 summarizes the method, data, and models used in this study. They are described in the following sections.

2.1 Method of creating the earthquake ground motion evaluation model

Various machine-learning methods have been proposed. After conducting preliminary studies using various methods to obtain highly accurate and stable evaluation results, the gradient boosting decision tree[16)] method, a method combining the gradient boosting and the decision tree methods, was used as the machine learning method. Figure 1 illustrates the concept of the gradient boosting decision tree. The gradient boosting process is a method of constructing a strong classifier (high-performance machine-learning model) by combining multiple weak classifiers (low-performance machine-learning models).

Table 1　Method, data, and models

Machine learning method	Gradient boosting decision tree
Earthquake motion data used for analyses	NS and EW components at K-NET observation stations of NIED
Earthquake motion indices (Target Variables) used for analyses	Peak ground acceleration PGA [cm/s^2] Pseudo velocity response spectra ${}_{\mathrm{P}}S_{\mathrm{V}}(T)$ [cm/s] Velocity response duration time spectra $TS_{\mathrm{V}}(T)$ [s] * Period T = 0.1, 0.5, 1, 3, 5 [s], Damping factor h = 0.05 * Parameters of TS_{V}: $p1$ = 0.03, $p2$ = 0.95 * $\log_{10} PGA$ and $\log_{10}{}_{\mathrm{P}}S_{\mathrm{V}}$ are used for analyses
Feature parameters used for analyses	Moment magnitude M_{W} Hypocentral depth H [km] Hypocentral distance X [km] Epicentral direction Λ [degree] * $\sin\Lambda$ and $\cos\Lambda$ are used for analyses

Earthquake motion model	Dataset	Station	Earthquakes	Records
Model S	Dataset S	SIT006	734	1468
Model T	Dataset T	TKY028	657	1314

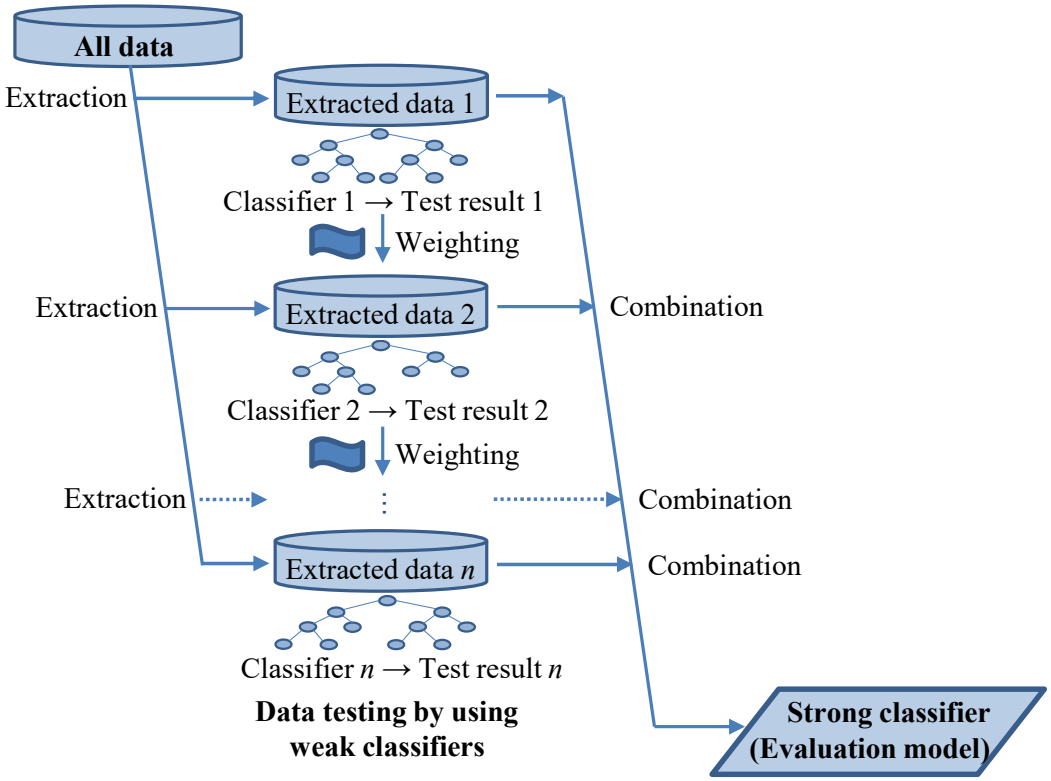

Fig. 1　Schematic explanation of the gradient boosting decision tree

The decision tree is a method for creating a machine learning model that can perform classification and regression by conditional branching using the branch structure of a tree. The method of combining weak classifiers created by the decision tree by applying the gradient boosting process is called the gradient boosting decision tree method. In this study, eXtreme Gradient Boosting (XGBoost)[17] implemented in DataRobot[18] was selected as the machine learning tool.

Eighty percent of the training dataset was divided into five parts. Four of these (64% of the training dataset) were used as teaching data for model creation, and one was used as validation data for evaluating the accuracy of the model. A cross-validation test was performed with five repetitions. The remaining 20% of the dataset was used as test data to evaluate the generalizability of the model. Teaching, validation, and test data were selected randomly. An early stopping technique was applied to avoid overfitting.

2.2 Observation records and indices of earthquake ground motions used in the study

In this study, from the observation stations in the Kanto region of the strong motion seismograph network K-NET[1] of the National Research Institute for Earth Science and Disaster Resilience (NIED), stations SIT006 (Chichibu) and TKY028 (Etchujima) were selected. SIT006 is located on shallow bedrock and hard surface ground, and TKY028 is located on deep bedrock and soft surface ground. The earthquake ground motion evaluation models at these sites, called Model S for SIT006 and Model T for TKY028, were studied.

After a data search and download from the K-NET[1] website, every horizontal earthquake ground motion recorded at the aforementioned stations from 1996 to May 31, 2019, with a combined three-component peak ground acceleration displayed on the website of 1 cm/s^2 or more was selected. The ground motion data of earthquakes with seismic moment M_W obtained by the broadband seismograph network F-net[19] of NIED were selected and used as training data for machine learning.

Figure 2 shows the epicenters of the target earthquakes[20] along with the locations of the observation stations[1] used in this study. The selected horizontal ground motions had a total of 1468 time histories (two components of each observation record of 734 earthquakes) at SIT006 and a total of 1314 time histories (of 657 earthquakes) at TKY028.

As earthquake motion indices for each component of each earthquake ground motion, which are the target variables of the machine learning when constructing an earthquake ground motion evaluation model, the peak ground acceleration PGA [cm/s^2], pseudo velocity response spectra ${}_pS_V$ [cm/s] and velocity response duration time spectra TS_V [s] [14] (period T = 0.1, 0.5, 1, 3, 5 [s], and damping factor h = 0.05) were calculated and examined, respectively. The parameters that defined the beginning and end of the response duration time were $p1$ = 0.03 and $p2$ = 0.95 [14].

2.3 Feature parameters of earthquake ground motion evaluation models

In this study, because an earthquake ground motion evaluation model specific to each site was created, the site effects among the three characteristics of source, propagation, and site were common within each site. Therefore, various internal studies, including trial and error assessment, were performed in advance to determine the feature parameters of the earthquake ground motion evaluation model. Four types of parameters were considered: moment magnitude, M_W, hypocentral depth, H [km], hypocentral distance, X [km], and epicentral direction, Λ [degrees]. These parameters describe the source and propagation characteristics and are considered to be physically independent of each other. M_W is the value obtained from the broadband seismograph network F-net[19] of NIED. The location of the hypocenter necessary for determining H, X, and Λ was obtained from data from the Japan Meteorological Agency[20], and the spread of the earthquake source fault was not considered. The observation station location data were obtained from the K-NET data[1]. Λ was set to 0° to due north and was defined clockwise. Because Λ becomes discontinuous at due north, the pair of sin Λ and cos Λ was input as feature parameters for the analyses. In this study, two components of ground motion (NS and EW components) were treated as data of horizontal ground motions. The difference in characteristics attributable to these components is beyond the scope of this study.

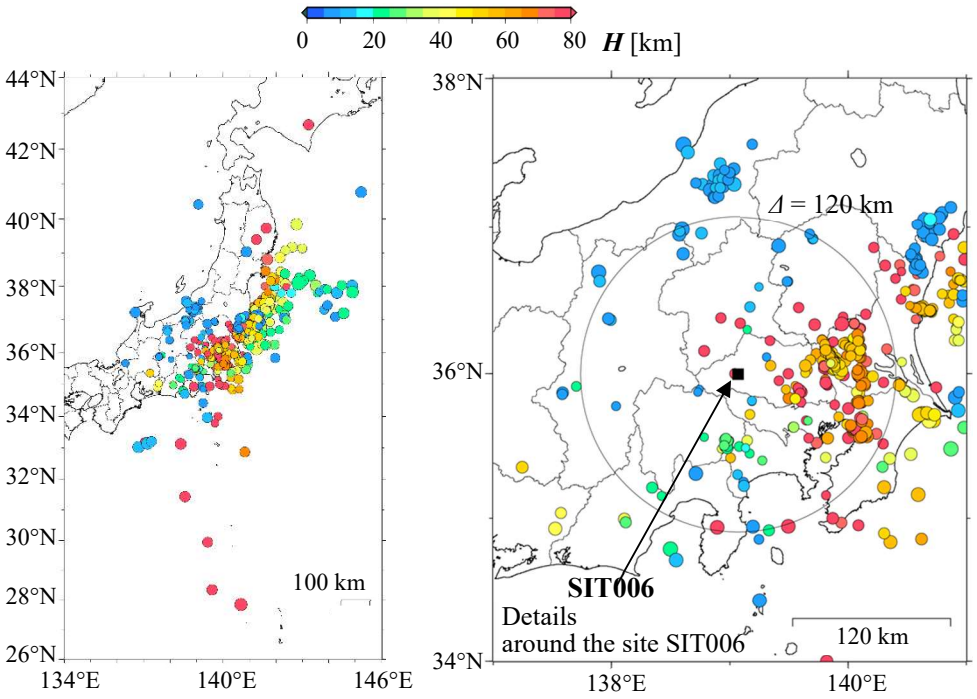

(a) Data for Model S

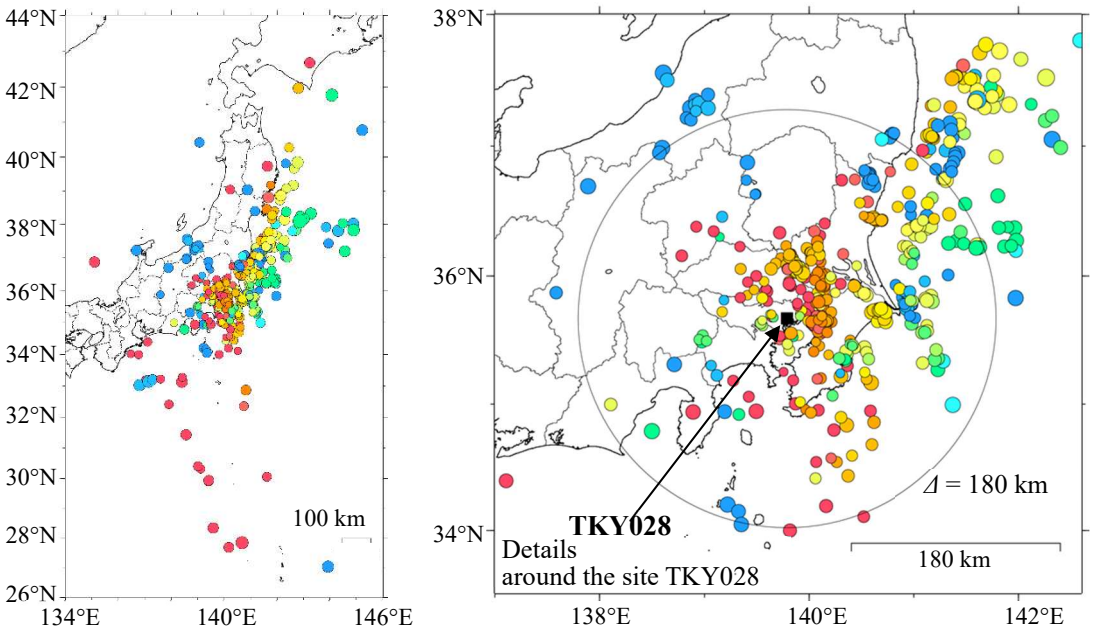

(b) Data for Model T

Fig. 2 The epicenters of the target earthquakes along with the locations of the observation stations used in this study

To avoid data with different target variables even though the feature parameters were exactly the same, an internal study was also conducted separately by adding the difference in the two components of the horizontal ground motion to the feature parameters. Because there was no significant difference in the results of that study[21], in this study, the same earthquake ground motion index was used without distinguishing between the two components as feature parameters.

When analyzing a model, it is necessary to investigate the effect of each feature parameter on the target variable. In this study, one feature parameter was selected from the data group used for machine learning. Then, only that data string was shuffled, replaced with a random data string, and the target variable was evaluated with the other feature parameter data strings unchanged. The degree to which the evaluation accuracy deteriorated at that time was defined as the feature impact. In the machine learning tool DataRobot[18], the feature impact is displayed as "Impact," calculated as Permutation Importance[22]. If the evaluation accuracy deteriorates significantly, the feature parameter is important. Conversely, if the evaluation accuracy does not change, the feature parameter does not affect the evaluation and is useless. In this study, none of the values were negative.

2.4 Machine learning model and its input data

Dataset S was the training dataset of the feature parameters and target variables required for machine learning to create Model S, the earthquake ground motion evaluation model for SIT006. Similarly, dataset T was the training dataset for creating Model T for TKY028.

Figure 3 shows examples of statistical correlations (scatter plots) of representative feature parameters and target variables of datasets S and T.

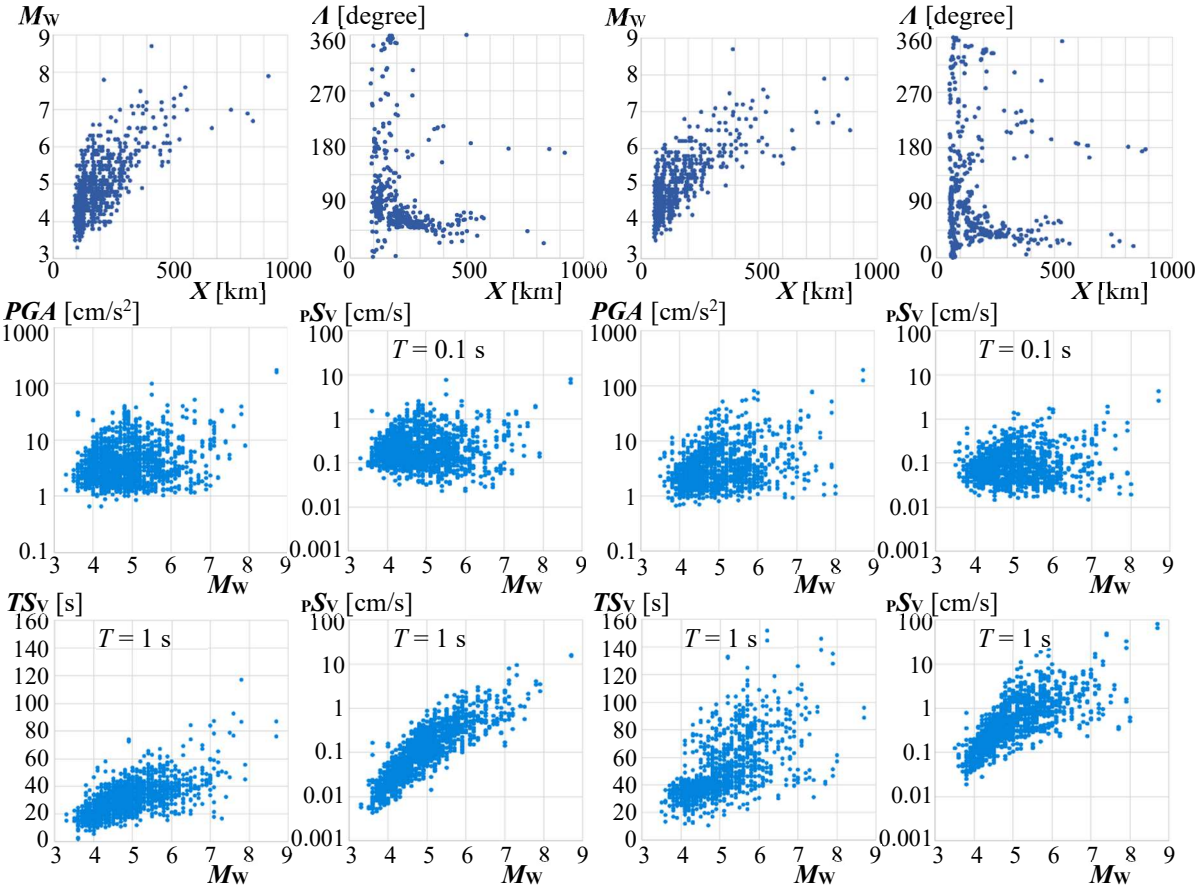

(a) Dataset S (b) Dataset T

Fig. 3 Examples of the relationship between the obtained data for feature parameters and the target variables of the earthquake ground motion evaluation models

There are only a few records of distant, small earthquakes. Even if epicenters were near, there were few earthquake data of very short distances, considering their hypocentral depths. Although the epicenters were in all directions, many were distributed in the northeast direction (approximately 45°), where many aftershocks of the 2011 off the Pacific Coast of Tohoku earthquake[20] occurred. In addition, at least in these examples, the long-period ${}_pS_v$ and TS_v are statistically dependent on the magnitude in contrast to the PGA and short-period ${}_pS_v$. In particular, in TKY028, which has deeper bedrock and is covered with softer sedimentary layers than SIT006, ${}_pS_v$ and TS_v in the long-period range become relatively larger with increasing M_W, and their scatter also becomes larger. This is thought to reflect the fact that when the scale of the earthquake is larger, the rupture area of the source fault is larger, the energy generated from the hypocenter is greater, the rupture time is longer, and the propagation paths of seismic waves, including surface waves, are more complex.

Figure 4 shows examples of histograms of the target variables of datasets S and T. Because there are few large data of PGA and ${}_pS_v$, these are transformed into common logarithmic data ($\log_{10} PGA$ and $\log_{10}$ ${}_pS_v$) to provide target variable data with distributions suitable for machine learning and to increase the precision of the earthquake ground motion evaluation model. For the loss functions used in the analyses, the least squares method (normal distribution) was applied to PGA and ${}_pS_v$, and the Poisson distribution was applied to TS_v.

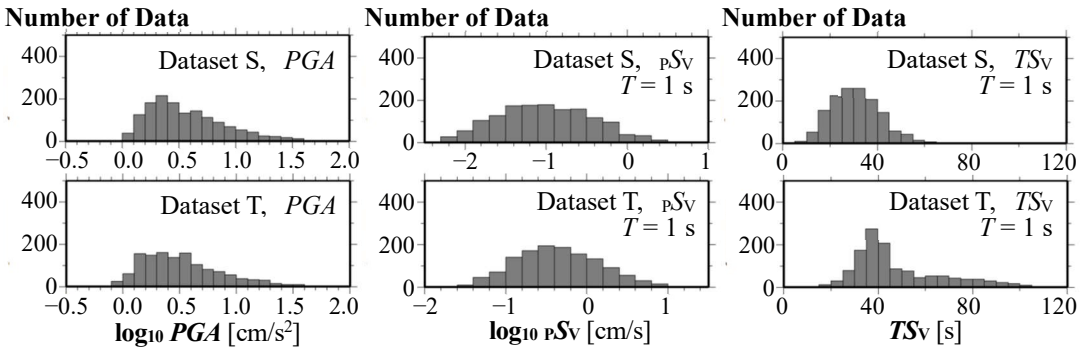

Fig. 4 Examples of histograms of the target variables

3. RESULTS

Models S and T were created by machine learning using datasets S and T, respectively.

3.1 Feature impacts on the earthquake ground motion indices (target variables)

The feature impacts on the earthquake motion indices (the target variables; PGA, ${}_pS_v$, TS_v) of Model S are shown in the left of Fig. 5. M_W and X have comparable impacts on PGA and short-period ${}_pS_v$ (the impact of X is slightly higher), but M_W has the greatest impact on other variables. The feature impacts of H are small. The feature impacts of Λ are greater in short periods than in long periods. The feature impact of Λ, which can be considered as the sum of the impacts of sin Λ and cos Λ in the figure, outweighs the impact of H, is larger for TS_v than for ${}_pS_v$, and outweighs the impact of X for periods shorter than 1 s.

The feature impacts on the earthquake motion indices of Model T are shown on the right side of Fig. 5. In short periods, the impacts of X are dominant; in other cases, the impacts of M_W are dominant. Generally, the feature impacts of M_W increase with period and those of X decrease with period. In comparison, the impact of H is not large, but its impact on TS_v in the long-period range is equal to or greater than that of X. The feature impacts of Λ are greater for TS_v than for PGA and ${}_pS_v$, exceed the impacts of X for periods other than 0.1 s, and even exceed the impacts of M_W in the short-period range.

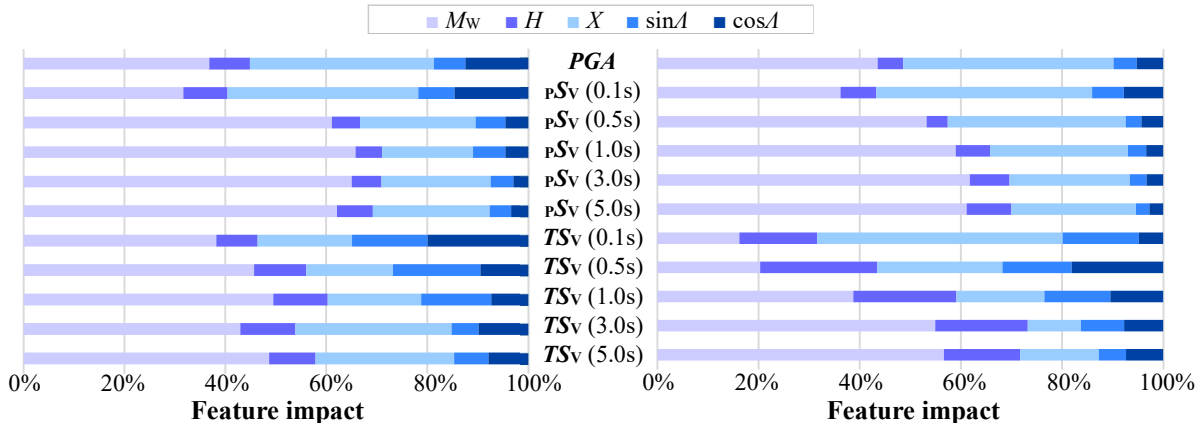

(a) Model S for SIT006 (b) Model T for TKY028

Fig. 5 Feature impacts on the earthquake motion indices (the target variables) of the earthquake ground motion evaluation models (the horizontal axis is normalized so that the total amount is 100%)

In addition, the impact of M_W on the short-period TS_v of Model T at Etchujima (TKY028), where the bedrock is deep, is smaller than that of Model S at Chichibu (SIT006), where the bedrock is shallow. To consider this point more generally, it will be necessary to perform a more detailed examination by selecting more records of earthquakes at more stations.

3.2 Comparison of observed and evaluated values for each earthquake ground motion index

The relationship between the observed and evaluated values for each earthquake ground motion index (target variable; *PGA*, ${}_pS_v$, TS_v) is shown in Fig. 6, with observed values on the horizontal axis and evaluated values on the vertical axis. As mentioned above, for *PGA* and ${}_pS_v$, the respective common logarithms ($\log_{10}$ *PGA* and $\log_{10}\,{}_pS_v$) are given as the target variable data for analysis. There is no significant difference between the distribution of teaching and validation data (indicated by black marks) and the distribution of test data (indicated by red marks). The observed values are well evaluated and modeled for all teaching, validation, and test data, and most of the evaluation values are in the range of twice to half the observed values. Looking at the results in detail, there is slight underestimation for large amplitudes, slight overestimation for small amplitudes, and slight overestimation for short duration times, with a slightly large variation.

Furthermore, examples of histograms of the ratios of the evaluated earthquake motion indices to the observed indices are shown in Fig. 7, and their averages and variations are listed in Table 2. The ratios of the evaluated earthquake motion indices to the observed indices have a relatively uniform distribution centered at approximately 1, and the variations in response duration time are smaller than those in amplitude (maximum values and response spectra). Overall, the observed values are evaluated and modeled well, and most of the evaluated values are within twice (2 on the horizontal axis) to half (0.5 on the horizontal axis) the observed values. As shown in Table 2, the averages of the ratios of the evaluated earthquake motion indices to the observed indices are almost 1; therefore, the averages of the common logarithms of the ratios are approximately 0. The averages of the common logarithms of the ratios of the evaluated earthquake motion indices to the observed indices are slightly greater than 0.2 in the amplitude, equal to or less than the values obtained in previous studies[e.g.2)]. This study is the first analysis example of response duration time. There is no previous statistical analysis case as there is for amplitude. Additionally, it should be noted that the physical meaning is different from the amplitude. However, in the results of this study, the observed values are evaluated and modeled better than those of amplitude, and the common logarithms of the ratios of the evaluated values to the observed values are slightly more than 0.1. At the shortest period (0.1 s), the variation is somewhat large.

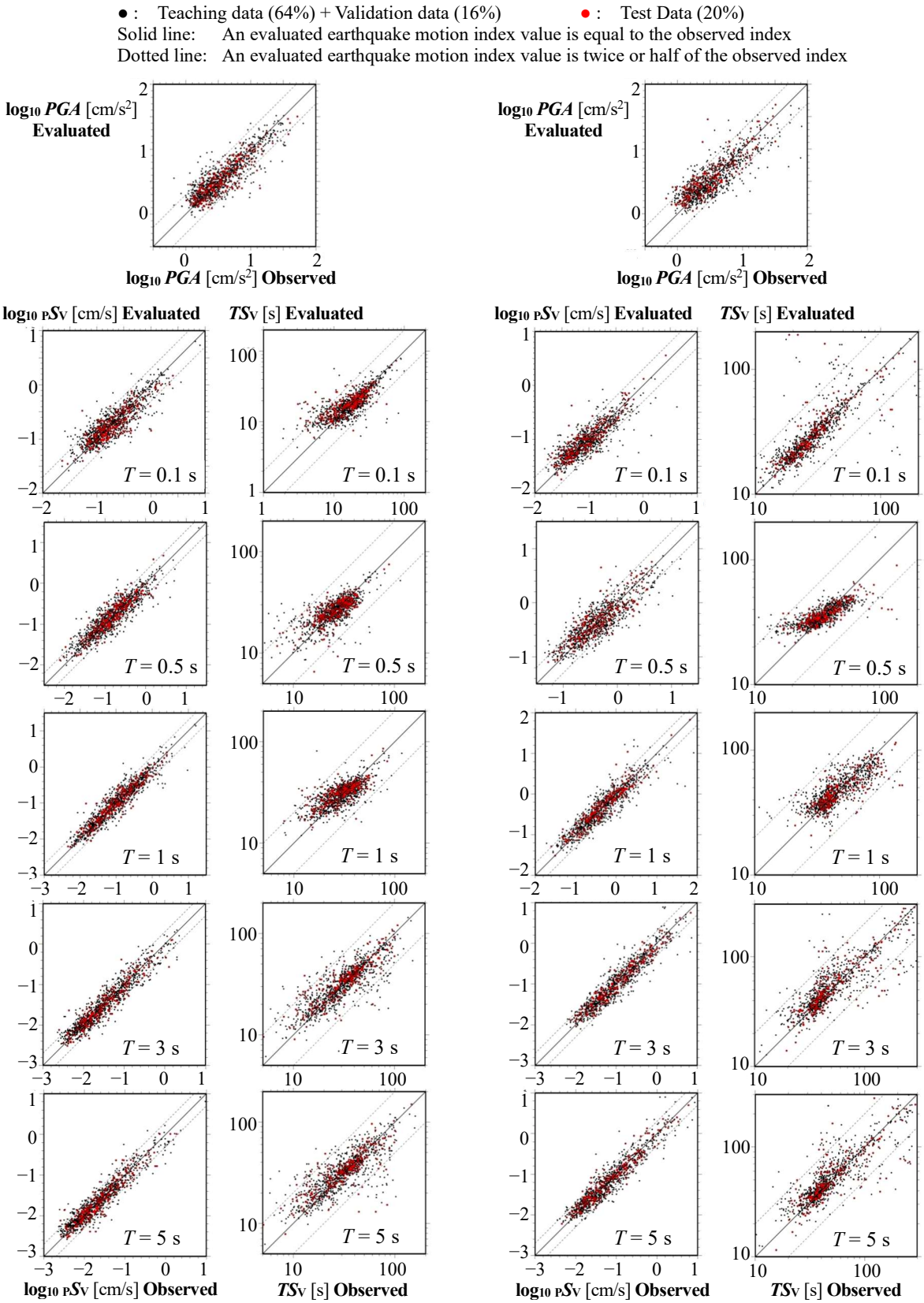

(a) Model S for SIT006 (b) Model T for TKY028

Fig. 6 Examples of relationship between the observed target variable values ($\log_{10} PGA$, $\log_{10} pSV$, TSV) and the evaluated target variable values (period T [s], damping factor 0.05)

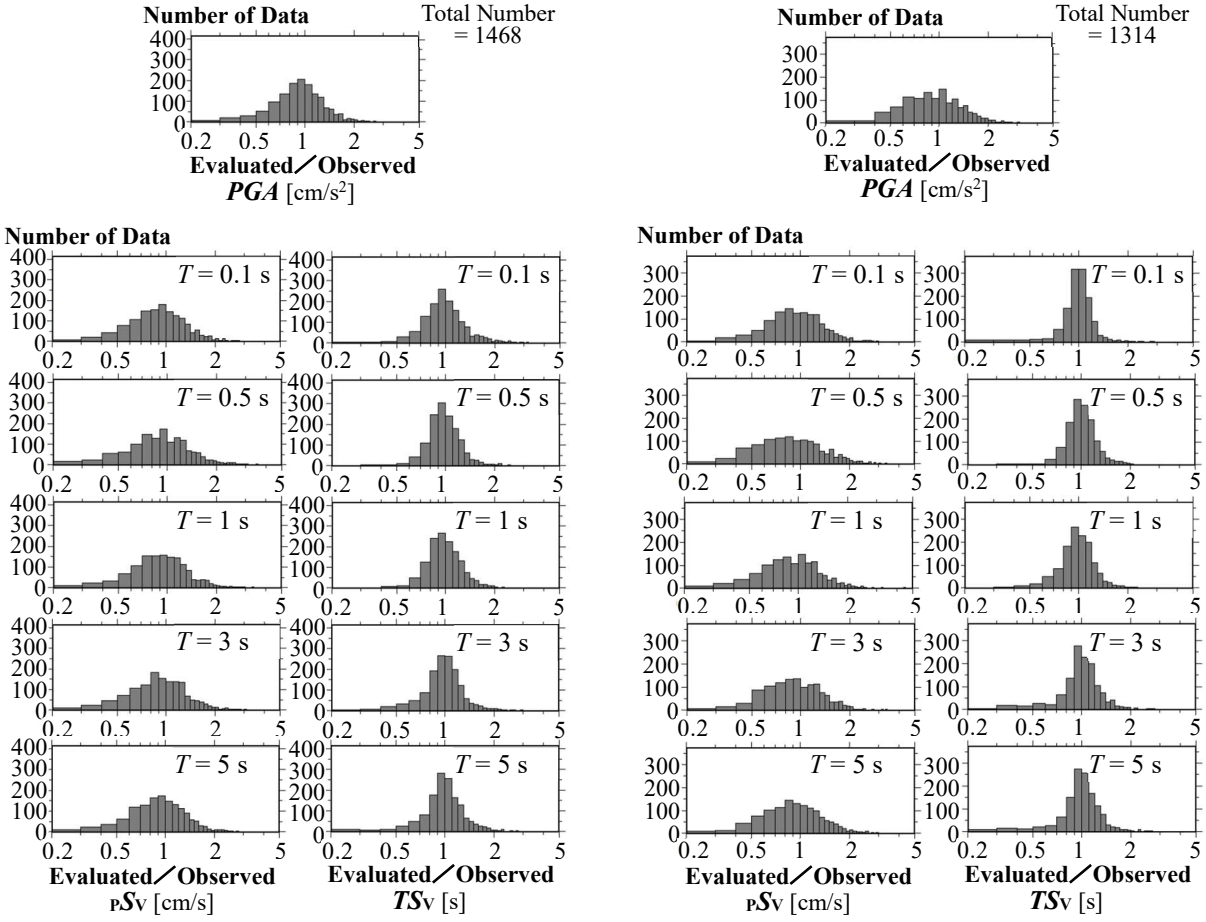

(a) Model S for SIT006　　(b) Model T for TKY028

Fig. 7　Examples of histograms of the ratios of the evaluated earthquake motion indices (*PGA*, $_{P}S_{V}$, TS_{V}) to the observed indices (period T [s], damping factor 0.05)

Table 2　Ratios of the evaluated earthquake motion indices (*PGA*, $_{P}S_{V}$, TS_{V}) to the observed indices

Earthquake motion index	***PGA***	**$_{P}S_{V}$**					**TS_{V}**				
Period [s]	—	0.1	0.5	1	3	5	0.1	0.5	1	3	5
Average of ratios of the evaluated to the observed											
Model S (SIT006)	1.08	1.10	1.14	1.11	1.09	1.09	1.16	1.06	1.07	1.09	1.10
Model T (TKY028)	1.15	1.15	1.16	1.14	1.13	1.13	1.09	1.07	1.06	1.09	1.09
Common logarithmic average of ratios of the evaluated to the observed											
Model S (SIT006)	0.00	0.00	0.01	0.00	0.00	0.00	0.03	0.01	0.01	0.01	0.02
Model T (TKY028)	0.01	0.02	0.00	0.01	0.00	0.00	0.01	0.02	0.01	0.02	0.01
Common logarithmic standard deviation of ratios of the evaluated to the observed											
Model S (SIT006)	0.19	0.22	0.25	0.22	0.21	0.21	0.19	0.12	0.13	0.15	0.16
Model T (TKY028)	0.20	0.20	0.23	0.21	0.20	0.20	0.15	0.11	0.11	0.14	0.14

3.3 Epicentral direction dependency of the evaluated value of each earthquake motion index

The epicentral direction dependency of each evaluated earthquake motion index (PGA, ${}_pS_v$, TS_v) was investigated.

Figure 8 shows examples (${}_pS_v$, TS_v) of the epicentral direction dependency of the evaluated earthquake motion indices, which are normalized by the maximum values calculated in 72 directions in five-degree increments. Model S results with $M_W = 5$, $H = 10$ km, and $X = 120$ km are shown on the left, and model T results with $M_W = 6$, $H = 10$ km, and $X = 180$ km are shown on the right. The calculation conditions shown here were selected as study examples based on the distribution of multiple shallow crustal earthquakes (mainly shown in blue) in multiple directions (north-northwest, south-southwest, and northeast, etc.) (Fig. 2).

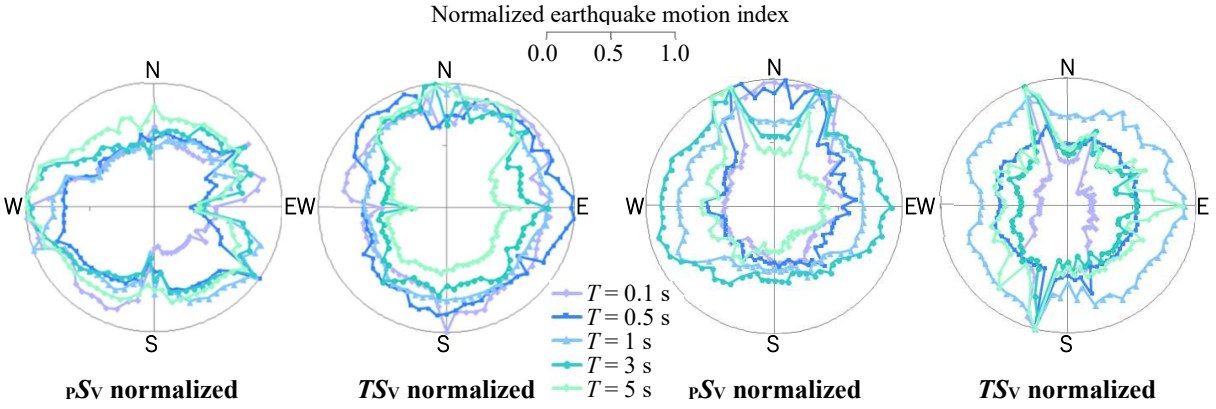

(a) Model S for SIT006
($M_W = 5$, $H = 10$ km, $X = 120$ km)

(b) Model T for TKY028
($M_W = 6$, $H = 10$ km, $X = 180$ km)

Fig. 8 Examples (${}_pSV$, TSV) of the epicentral direction dependency of the evaluated earthquake motion indices normalized by the maximum values calculated in 72 directions in 5-degree increments (period T [s], damping factor 0.05)

Figure 9 shows examples ($M_W = 6$, $H = 10$ km, $X = 180$ km) of the epicentral direction dependency of the evaluation values (raw values) of the pseudo-velocity response spectra ${}_pSV$ and the velocity response duration time spectra TSV. The ${}_pS_v$ results are shown in the upper row, and the TS_v results are shown in the lower row. These examples show the epicentral direction dependency of earthquake ground motion, and the characteristics differ depending on the site and period, as well as between ${}_pS_v$ and TS_v. For example, in the case of events in the north-northwest direction, especially in the long-period range, both ${}_pS_v$ and TS_v show large values. In the deep underground structure in the Kanto region and its surroundings[23], a deep channel-like bedrock structure continues from the direction of Niigata Prefecture to central Tokyo. The aforementioned epicentral direction dependency may reflect the excitation and propagation of surface waves due to such deep subsurface structures. In addition, as shown in Fig. 9, the absolute values of both ${}_pS_v$ and TS_v are larger for Model T than for Model S in most cases. Because the basement is deep in central Tokyo and covered with soft sedimentary layers in mainly the Tokyo Bay area, it seems that the seismic site characteristics of TKY028 are greater than those of SIT006.

Next, Fig. 10 shows study examples (Model T, $M_W = 6$, $H = 10$ km, $X = 180$ km) on how to provide epicentral directions in machine learning. Examples of the examination of the contribution to Model T of sin Λ and cos Λ, which are provided as feature parameters of the epicentral direction in machine learning, are shown at the top of Fig. 10. The results using only sin Λ are north–south symmetric (EW axis symmetric), and the results using only cos Λ are east–west symmetric (NS axis symmetric).

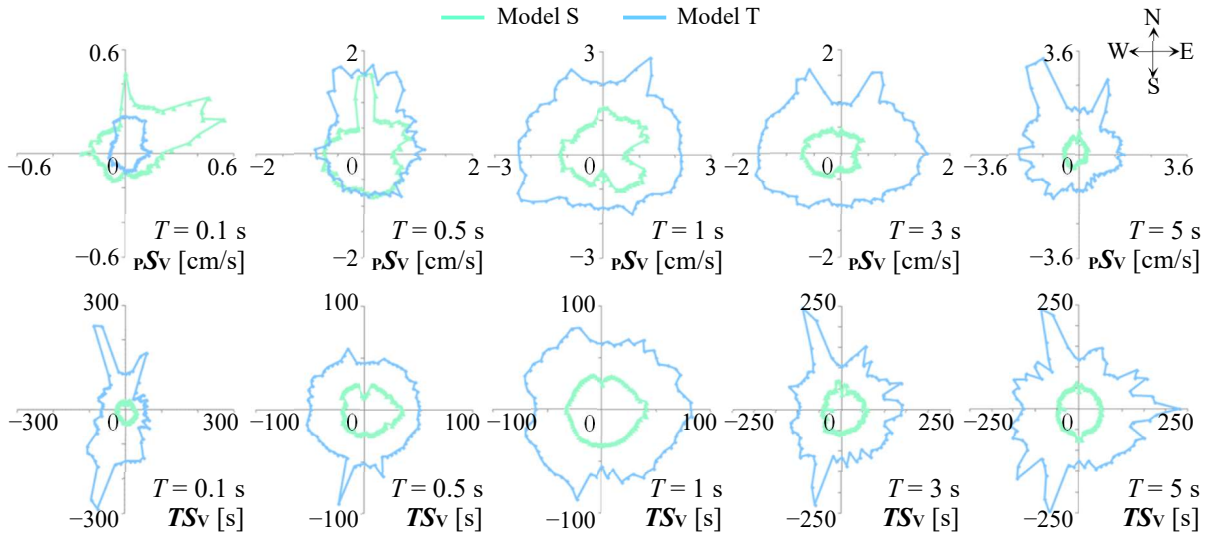

Fig. 9 Examples ($_{P}S_{V}$, TS_{V}) of the epicentral direction dependency of the evaluated earthquake motion indices calculated in 72 directions in 5-degree increments (period T [s], damping factor 0.05, $M_{W} = 6$, $H = 10$ km, $X = 180$ km)

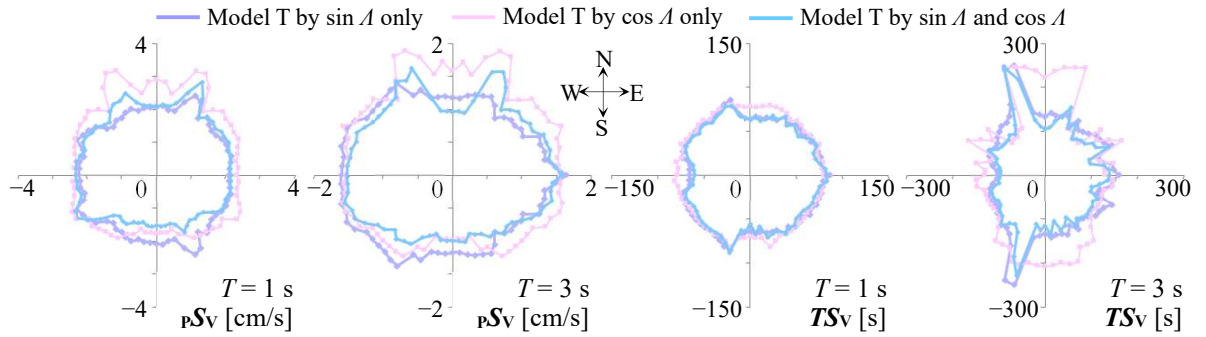

(a) Studies on the contribution of sine and cosine functions of epicentral directions to Model T

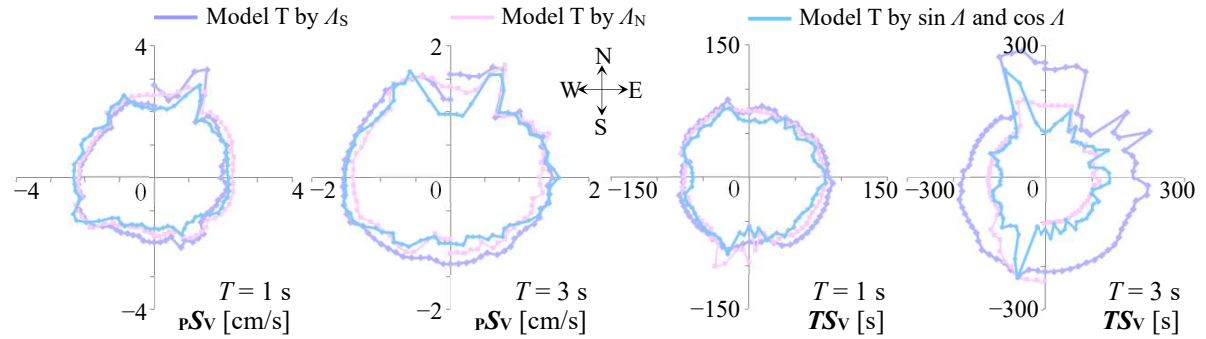

(b) Studies on the effect of epicentral directions of zero degrees in Model T (the zero-degree direction is due north for $\Lambda_{S} = \Lambda$ and due south for Λ_{N})

Fig. 10 Studies on modeling methods of epicentral directions for machine learning (Model T, period T [s], damping factor 0.05, $M_{W} = 6$, $H = 10$ km, $X = 180$ km)

Examples of studies on the effect of the epicentral direction of zero degrees ($\Lambda = 0°$) on Model T are illustrated at the bottom of Fig. 10. The zero-degree epicentral direction is due north for Λ_S, which is the same as Λ, and due south for Λ_N. The calculation result of the model becomes discontinuous in the zero-degree epicentral direction ($\Lambda = 0°$). Results with a period of 3 s are more variable than those with a period of 1 s. Among the results of TS_V with a period of 3 s, the absolute values obtained by the model using Λ_S are larger than those of the others, approximately twice as large in many directions. However, in the north-northwest, south-southwest, and northeast directions where the training data exist, the results of these models are almost the same. In the directions and regions where there are insufficient training data, the reliability of the model may be low due to insufficient training.

3.4 Investigation of method to provide epicentral directions as feature parameters and the effects

There are several ways to learn epicentral directions. Herein, Case C10 is the basic Model T described thus far, that is, the case in which the epicentral direction Λ is determined clockwise with due north at 0°, and the pair of sin Λ and cos Λ is applied to actual machine learning. In addition, cases in which the epicentral directions are provided in other various ways (see the upper part of Fig. 12, which will be described later) were also set. This section examines these cases, how to provide the epicentral direction, and its effects.

First, as described in the previous section, cases in which only sin Λ and cos Λ are given as feature parameters for the epicentral directions were set. These are referred to as Case C11 and Case C12, respectively. In addition, Case C01, which uses Λ_S (same as Λ above) as feature data and defines due north as the 0° epicentral direction, and Case C02, which uses Λ_N as feature data and defines due south as the 0° epicentral direction, were also set. Case C01 for the northern earthquakes and Case C02 for the southern earthquakes may have poor evaluation accuracy because the values of the epicentral directions are discontinuous near the epicentral direction of 0°.

As shown in Fig. 2, the epicentral distribution of earthquakes is not uniform, so the reliability of the evaluation results may vary greatly depending on the amount of training data around the evaluation target. Therefore, as the feature parameters of the epicentral directions, instead of a continuous quantity corresponding to the epicentral direction of each earthquake, four cases (C21 to C24) provided with the corresponding categories among the 12 preset directions (herein called the "category of epicentral direction"), were also established. In C24, four sets of numbers corresponding to the numbers of occurrences of the four directions, N, S, E, and W, in the string of C22 are provided. Case C33, in which the 12 categories of epicentral directions of C23 was increased to 20 categories, was also established.

Figure 11 shows the feature impacts (period 3 s, damping factor 0.05) in each case of Model T with different methods of providing the feature parameters of the epicentral directions. The trend is common for each case; however, in the five cases (C21 to C24, C33) with categories of epicentral directions, the feature impacts on the epicentral directions are relatively small. Therefore, training individual epicentral direction data rather than categories of epicentral directions may reflect epicentral direction characteristics in the evaluation results more effectively. However, it should be noted that whether it is appropriate depends on how the feature impact is evaluated and how the model is utilized.

Figure 12 shows examples of the epicentral direction dependency of the pseudo-velocity response spectra ${}_PS_V$ and the velocity response duration time spectra TS_V evaluated using a machine learning model under the conditions of $M_W = 6$, $H = 10$ km, and $X = 180$ km. For the five cases in which the feature parameters of the epicentral directions are given as a continuous quantity, values obtained at 5° steps were plotted; for the five cases where the categories of epicentral directions are given, the values obtained were plotted at the center of the corresponding categories. Because of the trigonometric functions used, the result for C11 has north–south symmetry, and the result for C12 has east–west symmetry. Although C01 is discontinuous due north and C02 is discontinuous due south according to the epicentral direction definition, the results aside from these points are relatively close to that of C10. However, the TS_V of C01 is excessive in almost all directions. The reason for this is currently unknown. The results of C21–C24, with 12 categories of epicentral direction, are insensitive to changes in epicentral direction, and the result of C33, with 20 categories, is similar. There is less variation in the evaluation results in the northeast direction than in the other directions for each case. This may reflect

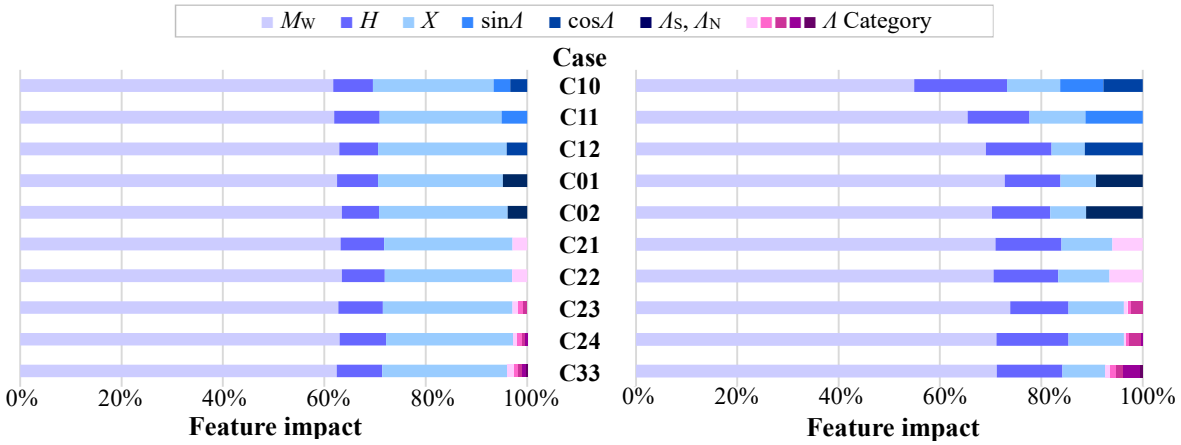

(a) Models for pseudo velocity response spectra ${}_{\mathrm{P}}S_{\mathrm{V}}$

(b) Models for velocity response duration time spectra TS_{V}

Fig. 11 Feature impacts in each case of the earthquake ground motion evaluation model T with different methods of providing the epicentral directions (period T = 3 s, damping factor 0.05, the horizontal axis is normalized so that the total amount is 100%)

the fact that there was an overwhelming amount of earthquake data in the northeast direction, as mentioned above. The observed earthquakes close to the evaluation conditions are mostly in the north-northwest and northeast directions, but there are some in the south-southwest direction. These epicentral direction characteristics are the characteristics observed in the evaluation results of C10. Conversely, there is a possibility that the reliability of the evaluation results is low in directions with few earthquakes that are close to the evaluation conditions.

4. DISCUSSION

In this study, considering the epicentral direction and the response duration time of the earthquake ground motion, which have not been addressed by conventional attenuation relations, an earthquake ground motion evaluation model specific to an observation site was created. Overall, the motion was evaluated and modeled well.

Among the target variables (earthquake ground motion indices) used in this study, the peak ground acceleration PGA is the maximum value of the earthquake ground motion, and the pseudo-velocity response spectrum ${}_{\mathrm{P}}S_{\mathrm{V}}$ is the maximum value of the response waveform reflecting strongly narrowband characteristics. Both are amplitude indices and are determined only by the maximum value that occurs at a certain moment in the time history. By contrast, the velocity response duration time spectrum TS_{V} is an index determined from the amplitude-squared cumulative curve of the entire response time history[14]. Such differences in character caused differences in the variability of each ratio of the evaluation value to the observed value, and TS_{V} seemed to be evaluated with less variability than PGA or ${}_{\mathrm{P}}S_{\mathrm{V}}$. TS_{V} seems to be an index that stably captures the temporal characteristics of the time history.

It is important to consider the differences in the earthquake ground motion characteristics depending on the epicentral direction. In particular, the influence of the epicentral direction Λ on TS_{V} is large, and in many cases, it is almost equal to or greater than the influence of the moment magnitude M_{W}, hypocentral depth H, and hypocentral distance X, which are considered in conventional prediction equations. These results reveal the possibility of evaluating the epicentral direction dependency of the amplitude and duration time of the earthquake ground motion according to the observation site and period. They are also useful for qualitative and quantitative analyses of various earthquake ground motion characteristics according to the location and period. Such a model can reflect the difference in the three-dimensional propagation characteristics of seismic waves relatively easily. In the past, these

Symbol	Case	Categories of epicentral direction	Number of feature parameters of epicentral directions	Method of providing feature parameters in each category of epicentral direction (clockwise from due south for C02, clockwise from due north for else)				
—◆—	C10	Continuous	2	$\sin \Lambda$, $\cos \Lambda$				
—◆—	C11	Continuous	1	$\sin \Lambda$				
—■—	C12	Continuous	1	$\cos \Lambda$				
—◆—	C01	Continuous	1	Λ_S (= Λ)				
—■—	C02	Continuous	1	Λ_N				
···◆···	C21	12 directions	1	1	2	3	…	12
—■—	C22	12 directions	1	NNN	NNE	NEE	…	NNW
—▲—	C23	12 directions	3	N, N, N	N, N, E	N, E, E	…	N, N, W
···✱···	C24	12 directions	4	3, 0, 0, 0	2, 0, 1, 0	1, 0, 2, 0	…	2, 0, 0, 1
—✱—	C33	20 directions	5	N,N,N,N,N	N,N,N,N,E	N,N,N,E,E	…	N,N,N,N,W

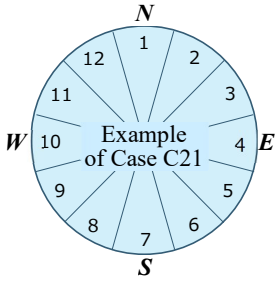

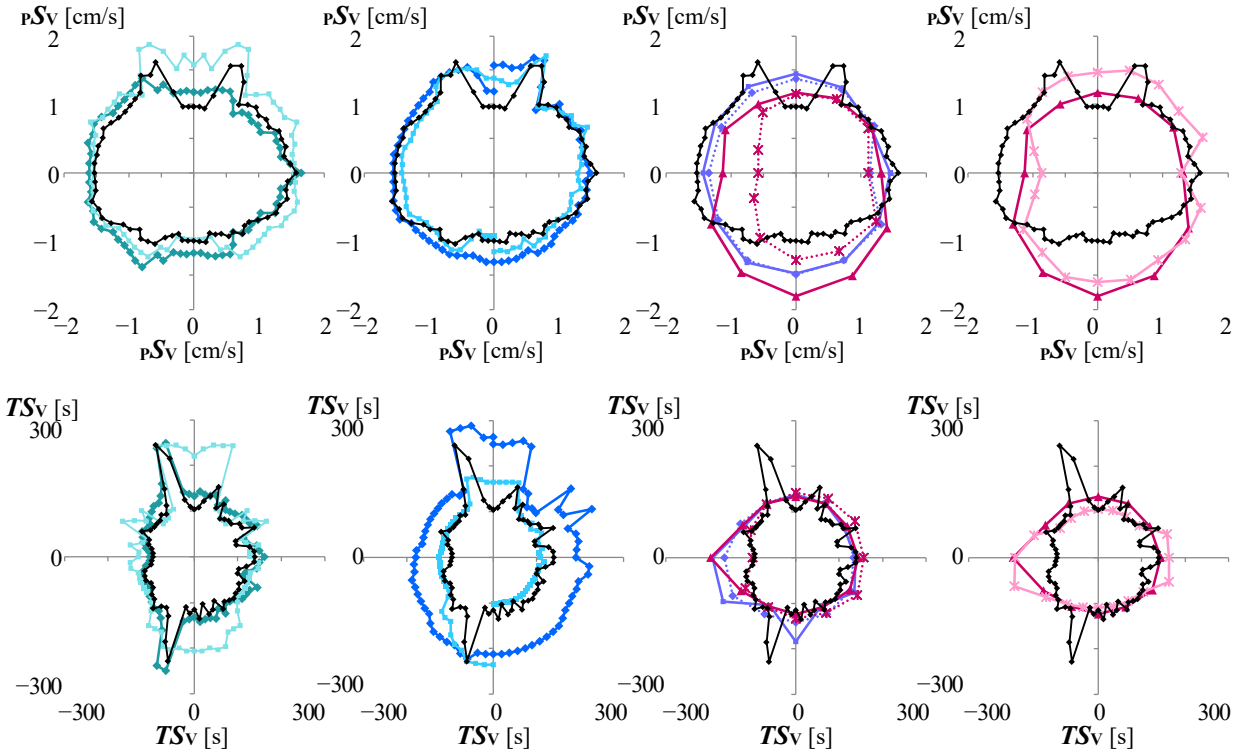

(a) Effect of sine and cosine of epicentral direction

(b) Effect of epicentral direction of zero degree

(c) Effect of representation of categories of epicentral direction

(d) Effect of difference in number of categories of epicentral direction

Fig. 12 Examples of the epicentral direction dependency of the pseudo-velocity response spectra $_pS_V$ and the velocity response duration time spectra TS_V evaluated using a machine learning model (Model T, period T = 3 s, damping factor 0.05, M_W = 6, H = 10 km, X = 180 km)

could not be expressed adequately without a sophisticated and detailed method. Hereafter, it is necessary to proceed with the examination of the interpretation of the model and its evaluation results using individual observation records and surrounding subsurface structure information.

In addition, depending on how the epicentral direction Λ is learned, there is a risk that the evaluation results may be distorted or that the evaluation accuracy may be degraded. If sufficient data exist, it is better to make use of the raw data than to set categories of epicentral directions and organize them. Considering that the influence of the epicentral direction value discontinuity on the analysis should be

avoided, case C10 in this study, which applies the pair of sin Λ and cos Λ, is considered an appropriate method.

Looking at the results of this study in detail, it showed slight underestimation for large amplitudes, slight overestimation for small amplitudes, and slight overestimation with a slightly large variation for short duration times. In particular, it is necessary to devise methods to improve the imbalance in model accuracy caused by sparseness and fineness of the data. It is also necessary to consider extrapolation to areas of large earthquakes, large-amplitude ground motions, and long duration ground motions, for which data are overwhelmingly scarce. For this purpose, the weighting of data or utilization of earthquake ground motion evaluation results by existing methods, including ground motion prediction equations and fault models, can be considered. It is also necessary to consider how well the model can explain the observation records and existing knowledge, including the variations.

The number of earthquake ground motion observation records used for modeling at individual sites remains insufficient. If there are few observed earthquakes close to the evaluation conditions, the reliability of the earthquake ground motion evaluation results may be low. In this study, although the observed ground motion values appear to have been evaluated well as a whole, the overall evaluation could attain even higher quality if the latest data accumulated at each point could be utilized most effectively. As only two sites were examined in this study, it is necessary to increase the number of sites and examine and analyze these in the future. It is also necessary to examine sites other than sites in the Kanto region. In addition, although the topic was not considered here, the characteristics of the two horizontal components of the earthquake ground motion are not only different for each earthquake but also change with a lot of groups of seismic waves arriving, even within the time history of a single earthquake. Therefore, if this is to be discussed, it is necessary to analyze not only the earthquake ground motion index for the entire time history but also perform individual and detailed analyses. The vertical ground motions must also be considered.

In addition, it is important to examine and select data and to consider data from which adverse effects, such as long-period noise, have been carefully removed. In particular, when considering the effect on response duration time, it is important to examine and select the base data carefully[25]. In the future, it will be essential to develop and systematize primary processing methods such as automatic selection methods and automatic filter processing for base data to create earthquake ground motion evaluation models.

5. CONCLUSIONS

In this study, to acquire new knowledge by earthquake ground motion evaluation from a new perspective, the authors newly created an earthquake ground motion evaluation model unique to each seismic observation site by machine learning using earthquake ground motion records obtained in the past as training data. Specifically, two sites in the Tokyo metropolitan area were examined. The epicentral directions and response duration times of earthquake ground motions, which have not been addressed in conventional attenuation relations, were also considered. Overall, the observed values were evaluated and modeled well, and the ratio of the evaluated values to the observed values showed a well-defined distribution centered on 1, with most of the evaluated values falling within the range of twice to half of the observed values. Expressing the scatter of the ratio of the evaluation value to the observed value by the common logarithmic standard deviation, in the case of the amplitude of the earthquake ground motion, the value was slightly exceeded 0.2, which is less than or equal to the existing result. On the other hand, in the case of the response duration time, which was newly considered here because there was no previous statistical analysis case, the value was even smaller, a little more than 0.1, and could be evaluated more accurately than the amplitude. The impact of the epicentral direction on the response duration time was large, in many cases equal to or greater than the effect of each parameter treated in the conventional ground motion prediction equations. However, it should be noted that the reliability of the evaluation results may be low when there are few earthquakes close to the evaluation conditions.

In the future, it will be necessary to make maximum use of big data nationwide and conduct studies using artificial intelligence (AI). If AI and big data can be used for earthquake ground motion evaluation,

it provides the great advantage that a large amount of data and high-quality information can be obtained, and an earthquake ground motion model specific to each location can be constructed by making the most of these data. If so, there is a high possibility of dramatically advancing analysis and discussion of differences due to hypocentral regions and observation areas or locations. It is expected that it will be possible to realize and improve the explainability of the AI examination process and examination results, which is currently difficult, by considering existing earthquake ground motion evaluation equations, evaluation results, and their physical conditions.

ACKNOWLEDGMENT

The current study utilized earthquake information from the Japan Meteorological Agency, the public data from the strong motion observation network of the National Research Institute for Earth Science and Disaster Resilience, and the machine learning platform "DataRobot." In addition, generic mapping tools (GMT) were used to create the epicentral distribution maps. The authors thank Mr. Kensuke Wada for his valuable opinions regarding this research while he was employed at the Shimizu Corporation, the anonymous reviewers for their valuable opinions on the manuscript, and Editage (www.editage.com) for English language editing. Certain portions of this study were published in References 24 to 27.

REFERENCES

1) National Research Institute for Earth Science and Disaster Resilience: *NIED K-NET, KiK-net*, 2019. https://doi.org/10.17598/NIED.0004
2) Morikawa, N. and Fujiwara, H.: A New Ground Motion Prediction Equation for Japan Applicable up to M9 Mega-Earthquake, *Journal of Disaster Research*, Vol. 8, No. 5, pp. 878–888, 2013.
3) Derras, B., Bard, P. Y., Cotton, F. and Bekkouche, A.: Adapting the Neural Network Approach to PGA Prediction: An Example Based on the KiK-net Data, *Bulletin of the Seismological Society of America*, Vol. 102, No. 4, pp. 1446–1461, 2012.
4) Kubo, H., Kunugi, T., Suzuki, S., Suzuki, W. and Aoi, S.: Construction of Ground Motion Prediction Equation Using Random Forest, *The 32nd Annual Conference of the Japanese Society for Artificial Intelligence*, 4Pin1-35, 2018 (in Japanese with English Abstract).
5) Kubo, H., Kunugi, T., Suzuki, S., Suzuki, W. and Aoi, S.: Attempt to Reduce the Effect of Biased Data-Set on Ground-Motion Prediction Using Machine Learning, *The 33rd Annual Conference of the Japanese Society for Artificial Intelligence*, 4K2-J-13-02, 2019 (in Japanese with English Abstract).
6) Kubo, H., Kunugi, T., Suzuki, W., Kimura, T. and Aoi, S.: Construction of Explainable Random Forest Predictor for Ground-Motion Intensity, *The 34th Annual Conference of the Japanese Society for Artificial Intelligence*, 4Rin1-94, 2020 (in Japanese with English Abstract).
7) Kubo, H., Kunugi, T., Suzuki, W., Suzuki, S. and Aoi, S.: Hybrid Predictor for Ground-Motion Intensity with Machine Learning and Conventional Ground Motion Prediction Equation, *Scientific Reports*, Vol. 10, 11871, 2020. https://doi.org/10.1038/s41598-020-68630-x
8) Ohno, S. and Tsuruta, R.: Ground-Motion Prediction by ANN Using Machine Learning for the Tohoku Region, Japan, *11th U.S. National Conference on Earthquake Engineering*, 998, 2018.
9) Matsuoka, K. and Ohno, S.: Examination of Spectral Evaluation of Seismic Motion Using Machine Learning, *Proceedings of the 15th Annual Meeting of Japan Association for Earthquake Engineering*, B-4-5, 2020 (in Japanese).
10) Okazaki, T., Morikawa, N., Iwaki, A., Fujiwara, H., Iwata, T. and Ueda, N.: Ground-Motion Prediction Model Based on Neural Networks to Extract Site Properties from Observational Records, *Bulletin of the Seismological Society of America*, Vol. 111, No. 4, pp. 1740–1753, 2021.
11) Ishii, T.: A Study on Response Duration Time Spectra of Earthquake Motions in Tokyo, *The 14th World Conference on Earthquake Engineering*, Beijing, China, 02-0020, 2008.

12) Arai, K., Ishii, T. and Hirata, N.: Study on Spatial Distribution of Response Duration Time of Earthquake Motions in Tokyo Metropolitan Area, *Proceedings of the Annual Meeting of Architectural Institute of Japan*, Vol. B-2, pp. 15–16, 2015 (in Japanese).
13) Ohsaki, Y.: *Spectral Analyses Guide of Earthquake Motion*, Kajima Institute Publishing Co., Ltd., 260 pp., 1981 (in Japanese).
14) Ishii, T.: Response Duration Time Spectra of Earthquake Ground Motions, *Journal of Structural and Construction Engineering (Transactions of AIJ)*, Architectural Institute of Japan, Vol. 77, No. 676, pp. 843–850, 2012 (in Japanese with English Abstract).
15) Japan Deep Learning Association: *Official Textbook for Deep Learning G (Generalist) Test*, Shoeisha Co., Ltd., 329 pp., 2018 (in Japanese).
16) Friedman, J. H.: Greedy Function Approximation: A Gradient Boosting Machine, *The Annals of Statistics*, Vol. 29, No. 5, pp. 1189–1232, 2001.
17) Chen, T. and Guestrin, C.: XGBoost: A Scalable Tree Boosting System, *Proceedings of the 22nd ACM SIGKDD International Conference on Knowledge Discovery and Data Mining*, pp. 785–794, 2016.
18) DataRobot. https://app.datarobot.com/ (last accessed on September 1, 2021)
19) National Research Institute for Earth Science and Disaster Resilience: *F-net*, 2019. https://www.doi.org/10.17598/NIED.0005
20) Japan Meteorological Agency: Earthquake Information (Earthquake and Seismic Intensity Information). http://www.jma.go.jp/en/quake/quake_singendo_index.html (last accessed on September 1, 2021)
21) Oana, A., Ishii, T. and Wada, K.: Applicability of Features to Ground Motion Evaluation Models Utilizing Machine Learning, *The 34th Annual Conference of the Japanese Society for Artificial Intelligence*, 3Rin4-03, 2020 (in Japanese with English Abstract).
22) Fisher, A., Rudin, C. and Dominici, F.: All Models are Wrong, but Many are Useful: Learning a Variable's Importance by Studying an Entire Class of Prediction Models Simultaneously, *Journal of Machine Learning Research*, Vol. 20, No. 177, pp. 1–81, 2019. https://arxiv.org/abs/1801.01489 (last accessed on September 1, 2021)
23) National Research Institute for Earth Science and Disaster Resilience: *J-SHIS*, 2019. https://doi.org/10.17598/nied.0010
24) Ishii, T., Oana, A. and Wada, K.: Study on Site-Specific Ground Motion Evaluation Models Utilizing Machine Learning Method Considering Epicentral Directions, *Programme and Abstracts, 2019 Fall Meeting*, The Seismological Society of Japan, S22-08, 2019 (in Japanese).
25) Ishii, T., Oana, A. and Wada, K.: Attempt to Acquire New Knowledge by Earthquake Ground Motion Evaluation Using Machine Learning, *Proceedings of the 14th Annual Meeting of Japan Association for Earthquake Engineering*, P1-13, 2019 (in Japanese).
26) Ishii, T., Oana, A. and Wada, K.: A Study on the Method of Giving the Epicentral Directions as Feature Parameters of the Ground Motion Evaluation Model by Machine Learning and its Effect, *Proceedings of the Annual Meeting of Architectural Institute of Japan*, Vol. B-2, pp. 195–196, 2020 (in Japanese).
27) Ishii, T., Oana, A. and Wada, K.: Study on Site-Specific Ground Motion Models Utilizing Machine Learning Considering Epicentral Directions, *Proceedings of the 17th World Conference on Earthquake Engineering*, Sendai, Japan, Version 2020, 1d-0010, 2020.

(Original Japanese Paper Published: May, 2022)
(English Version Submitted: April 13, 2023)
(English Version Accepted: May 8, 2023)